

Microneedle Gastric Retention for Drug Delivery

By

David Dellal

Submitted to the  
Department of Mechanical Engineering  
in Partial Fulfillment of the Requirements for the Degree of  
Bachelor of Science in Mechanical Engineering

at the

Massachusetts Institute of Technology

~~June 2017~~ [June 2018]

© 2017 David Dellal. All rights reserved.

The author hereby grants to MIT permission to reproduce and to distribute publicly paper and electronic copies of this thesis document in whole or in part in any medium now known or hereafter created.

Signature redacted

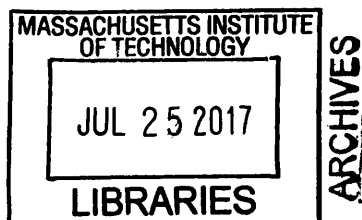
Signature of Author: \_\_\_\_\_  
Department of Mechanical Engineering  
May 10, 2017

Signature redacted

Certified by: \_\_\_\_\_  
Robert Langer  
David H. Koch Institute Professor  
Thesis Supervisor

Signature redacted

Accepted by: \_\_\_\_\_  
Rohit Karnik  
Professor of Mechanical Engineering  
Undergraduate Officer



# Microneedle Gastric Retention for Drug Delivery

By

David Dellal

Submitted to the Department of Mechanical Engineering  
on May 12, 2017 in Partial Fulfillment of the  
Requirements for the Degree of

Bachelor of Science in Mechanical Engineering

## **ABSTRACT**

Traditional drug delivery methods, such as injection and ingestion, are associated with many challenges, including patient needle-phobia and patient adherence to a medication regimen. Biologic molecules, in particular, must be injected due to degradation by enzymes in the GI tract. Previous scientists have developed a method with the potential to inject macromolecules in the GI tract using microneedles that can implant themselves in the stomach lining; however, they do not provide long-term drug delivery. To create a controlled release microinjection, I hypothesize that a hooked needle will latch onto the muscularis mucosae layer in the stomach and reside upwards of a week to deliver drugs. A number of trials and simulations have been designed to test the efficacy of this retention mechanism. Coupled with work in the creation of new pharmaceutical formulations, these needles can be loaded with any drug to ensure uptake into the blood stream over the course of several days.

Thesis Supervisor: Robert Langer

Title: David H. Koch Institute Professor

## TABLE OF CONTENTS

<b>Abstract</b>	2
<b>Table of Contents</b>	3
<b>List of Figures</b>	4
<b>1. Introduction</b>	5
1.1. Traditional Drug Delivery Methods	5
1.2. Anatomical Background	7
<b>2. Solution Overview</b>	9
2.1. Micropost Characterization	10
2.2. Computational Analysis of In-vivo Micropost Retention	13
<b>3. Experimental Verification of Micropost Retention</b>	18
3.1. Synthetic Stomach Experiment	18
3.2. In-vivo Trial Using Swine Model	20
<b>4. Conclusions and Future Work</b>	21
4.1. Conclusions	21
4.2. Future Experiments	22
4.3. Future Applications	23
<b>5. Acknowledgements</b>	25
<b>6. Bibliography</b>	25

## LIST OF FIGURES

<b>Figure 1.a.</b> Diagram of a GI tract	8
<b>Figure 1.b.</b> Histology of stomach lining	8
<b>Figure 2.a.</b> Diagram of self righting device to implant needle into the stomach	9
<b>Figure 2.b.</b> Hooked 32-gauge stainless steel needle	9
<b>Figure 2.c.</b> Hooked needle attached to muscle fibers of ex-vivo swine sample	9
<b>Figure 3.</b> Graph describing relationship of penetration depth and hooking force	11
<b>Figure 4.</b> Graph comparing penetration forces in swine and human stomach tissue	12
<b>Figure 5.</b> Computational model simulating drag forces from stomach flow	15
<b>Figure 6.</b> Computational model simulating gastric food effects	17
<b>Figure 7.</b> Illustration of the design of the fluid flow in-vitro experiment	19
<b>Figure 8.</b> Graph of the results of the in-vitro experiment testing drag effects	19

## **1. INTRODUCTION**

The aim of the research presented in this thesis is to understand the retentive capacity of microposts in the application of drug delivery. These may be used to deliver a range of pharmaceuticals, including biologic medications that traditionally must be injected.

The remainder of this chapter will discuss the traditional methods that are used for delivering medications, as well as provide a brief overview of the gastrointestinal (GI) tract. The second chapter provides an overview of the solution, as well as reports on preliminary results collected from ex-vivo experiments and computational simulations. Chapter 3 discusses further experiments that were conducted to verify the findings from the earlier tests. Lastly, Chapter 4 provides an overview of what can be deduced from these experiments, as well as describes several experiments that remain to be conducted and possible future applications.

### **1.1 Traditional Drug Delivery Methods**

One major factor that clinicians must consider when determining what medication to prescribe is the drug delivery method that must be used. Two of the most common options for delivering drugs are injection and ingestion. For many biologic drugs, injections must be used since these molecules are broken down by enzymes, such as pepsin, in the GI tract. Biologic drugs also have trouble diffusing through the epithelial barrier, comprised of closely packed cells, to reach the blood stream<sup>1</sup>. These biological barriers, coupled with the fact that many patients, such as children, are frightened by needles, make physicians reluctant to prescribe regular medications that require injection<sup>2 3</sup>. In addition, training is needed to perform needle injections through the skin, and many patients make mistakes while self-administering their dose. Lastly, improper disposal of needles often leads to injuries and increases the possibility of the

spread of infectious diseases, such as hepatitis and HIV<sup>4</sup>. Each year, problems with injections lead to 8-12 billion unsafe therapeutic injections causing over 1.3 million premature deaths and \$535 million in global medical costs<sup>5</sup>.

In order to compensate for these issues, doctors often prescribe medications that can be ingested orally by patients. However, these pills pose their own problems. Since many traditional medication capsules dissolve rapidly, the medications inside are quickly broken down by the body. Therefore, in order to maintain important drugs with short half lives in the body, patients are often required to regularly ingest their medications<sup>6</sup>. However, one of the greatest problems that clinicians face with oral delivery is patient adherence to a medication regimen. The percent of patients who adhere to their medical regimens can be as low as 37% for certain illnesses, which often exacerbate the existing issues. In addition, studies have also shown that reducing the number of pills required per day increases the patient compliance<sup>7</sup>.

In order to tackle this issue, gastrointestinal devices that can gradually delivery pharmaceuticals over time have shown great promise in mitigating this risk. These have taken various approaches from chemical to mechanical, such ion-exchange resin and micro-encapsulation respectively. However, due to low bioavailability of these formulations, the required dose is too high to be cost-effective for clinical applications. Drug-loaded, ingestible microneedles help solve several of these challenges associated with traditional drug delivery methods. However, while new methods have been developed with the potential to inject macromolecules in the GI tract using microneedles that implant themselves in the stomach lining, they currently do not provide long-term drug delivery<sup>8</sup>.

## 1.2 Anatomical Background

In order to create a device that can retain its position in the stomach lining, the anatomical structure and physiology of the organ must first be understood. In humans, as well as in several animals like pigs, the stomach lies at the end of the esophagus, a long fibromuscular tube that connects to the mouth where food enters the GI tract. The stomach, which is the primary location for food digestion in the human body, is a significant space that offers high residence times of 1-4 hours<sup>9</sup>. To digest the food, the stomach contains gastric acid that creates a low pH environment, as well as many enzymes, such as pepsin, that break it down into amino acids. Through muscular movements, the stomach exerts translational forces on its contents of roughly  $0.2 \text{ N}^{10,11}$ , which facilitates solution movement. Once food has sufficiently degraded, it passes through the pyloric sphincter into the duodenum to reach the small intestine. To protect itself from the harsh environment within, the interior surface of the stomach has a mucous coating that is 40 to 450  $\mu\text{m}$  thick. Under the mucosa lies the muscularis mucosa, a thin layer composed of smooth muscle fibers. The muscularis mucosa separates the mucosa from the submucosa, which covers the stomach's primary muscle fibers used for contraction. The stomach's location in the GI tract, as well as a histological sample that reveals the cross-section of the stomach lining, are shown in Figure 1.

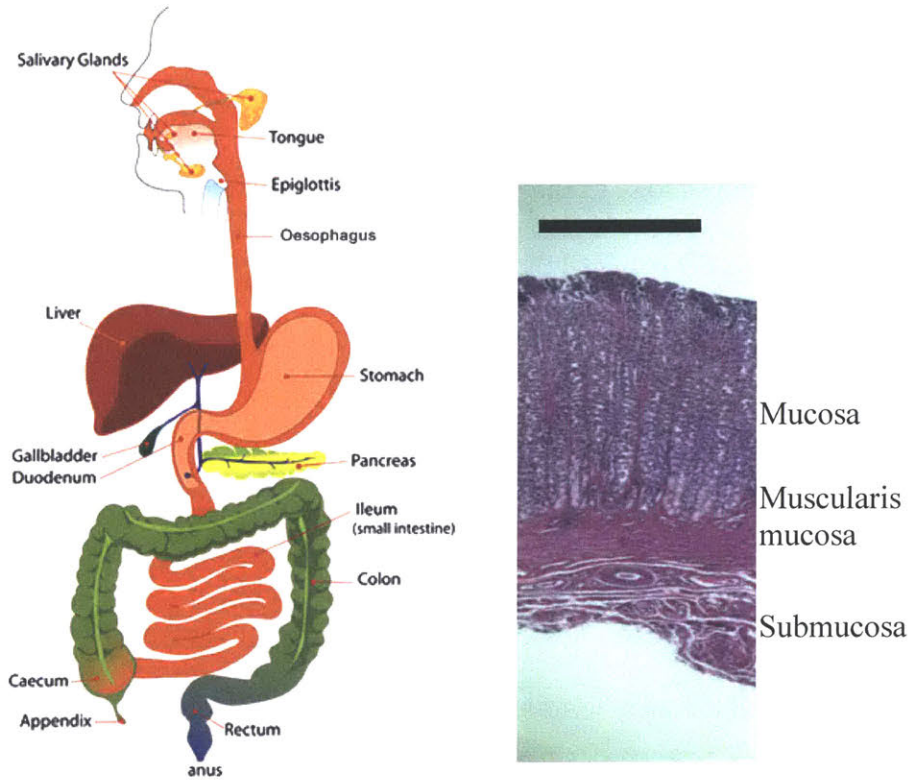


**Figure 1.** a. Diagram of the GI tract<sup>12</sup>. b. Stained histological sample that reveals three of the stomach lining's innermost layers in a pig (scale bar = 1 mm).



## 2. SOLUTION OVERVIEW

In order for the needle to penetrate the stomach lining, a system was designed to ensure its placement. Using the theory of a Gomboc<sup>13</sup>, a self-righting shape was previously designed so that the device can invert itself in the gastric acid with the needle facing down. The device itself is made of two different pieces, the heavier bottom piece is made of stainless steel, while the top piece is made out of polycaprolactone (PCL). In the center of the device sits the needle, which is attached to a sugarcoated, condensed spring. Once the sugar dissolves, the spring serves as an auto-injector that ejects the needle from the interior of the device so that it can insert itself into the muscle lining, as shown in Figure 2a. To increase the retention capacity of the needle, a force of 1N was exerted on the needle using an Instron machine to bend its tip, as shown in Figure 2b. This hook at the end of the needle was created to help the needle latch onto the muscle fibers in the distal stomach near the antrum, as shown in Figure 2c.

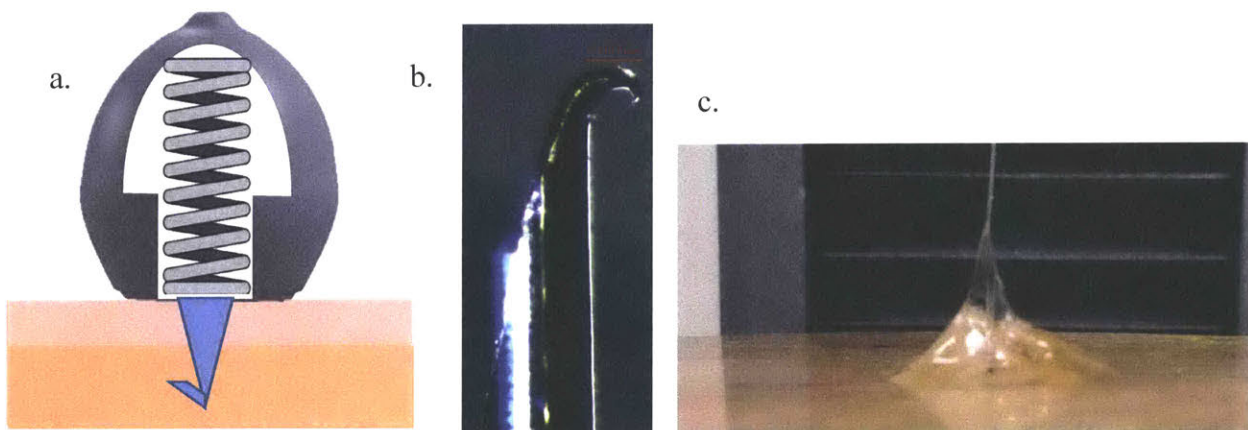


**Figure 2.** a. Diagram of the self righting device that was created to implant the needle in the stomach. The hooked needle has been inserted by the decompressed spring into the stomach lining b. A hooked 32-gauge stainless steel needle c. An image of a hooked needle that has attached itself to the muscle fibers of a tissue sample from a swine stomach.

## 2.1 Micropost Characterization

To determine the maximum force necessary to dislodge the needle from the stomach lining, an ex-vivo model was created using swine tissue since the pig's gastrointestinal tract has been shown to be a good model of its human counterpart<sup>14</sup>. In order to confirm this, an preliminary ex-vivo experiment was performed. To do so, a 10 cm by 10 cm section of tissue was dissected from the stomach of a Yorkshire pig. The swine tissue was then fixed between two acrylic plates, with the interior surface of the stomach facing up under the plate containing an approximate 3 cm diameter hole in its center. These plates were then placed on the Instron machine comprised of a moving arm containing a force sensor that is accurate up to 0.1 mN. On this arm of the Instron, a stainless steel hooked needle adhered to a screw was secured in place. To determine the force necessary to penetrate the tissue, the Instron arm was lowered at a constant rate of 0.1 mm/sec until it reached 5 mm of depth while the device recorded the hooking force required to be exerted to reach that layer. This experiment was then repeated using tissue from a human cadaver stomach. As shown in Figure 3, the human stomach exhibited very similar properties and produced almost equivalent results compared to the porcine trials.

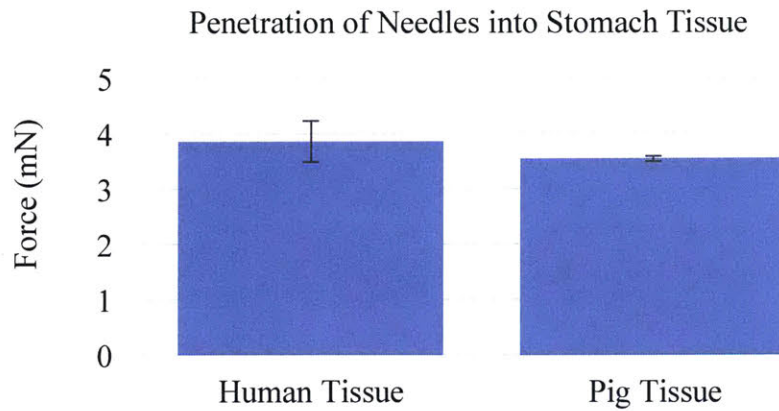


**Figure 3.** Graph comparing the forces required to penetrate a sample of human stomach tissue and its swine counterpart using stainless steel needles. Statistical analysis shows no significant difference.

With pig tissue proven to be a strong model for its human counterpart, a similar experiment was conducted to determine the ideal depth of penetration to maximize the retention force. To determine the ideal depth of penetration to maximize the retention force, the Instron arm was lowered at a constant rate of 0.1 mm/sec until it reached 1 mm, 3 mm, or 5 mm of penetration into the tissue. In this experiment, the Instron recorded the hooking force required to be exerted in order to reach that layer of penetration, as shown in Figure 4. From this analysis, it was confirmed that 2.5 mm of penetration were necessary to maximize the force.

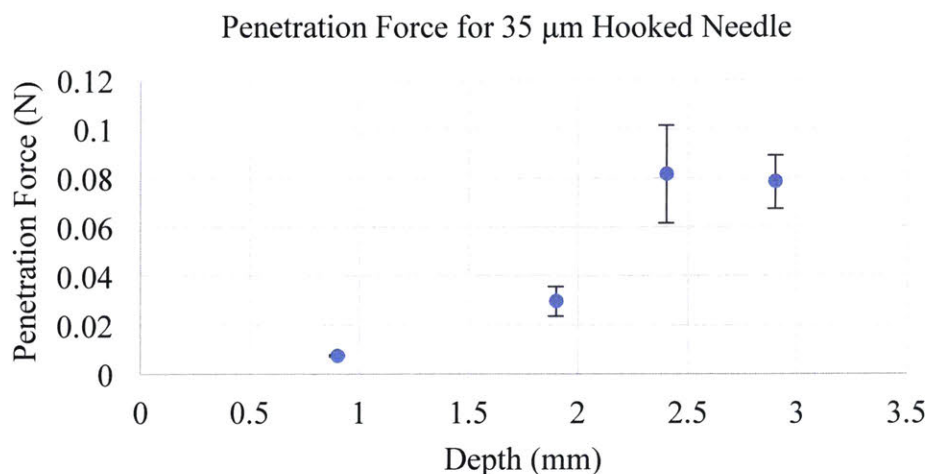


**Figure 4.** Graph describing the relationship between the penetration depth of a stainless steel needle into porcine tissue and the hooking force required to reach that layer.

In order to verify these measurements, as well as determine which layer of tissue maximized the hooking force, the needles were dyed with a surgical dye before use. Once the experiments were completed, the tissue was fixed to paraffin and sent to the Koch Institute for Integrative Cancer Research’s histology core. The needle puncture site was found by sectioning the tissue by making parallel lateral cuts every 10 microns. Once it was located, the site was analyzed under an inverted microscope to determine the penetration depth. These histology findings also confirmed that the needle had latched onto the muscle fibers in the mucosal musculae layer under the mucous in the stomach lining.

Lastly, to determine the force required to dislodge a needle anchored in the stomach lining, a similar experiment was conducted. A stainless steel hooked needle that was adhered to a screw was attached to the moving arm of the Instron. This arm was then lowered at a constant rate of 0.1 mm/sec until the needle penetrated 2.5 mm into fixed, fresh porcine tissue. Once this distance was reached, the arm was raised at a constant rate of 0.1 mm/sec until the needle detached from the tissue. Through this experiment, the Instron recorded the penetration depth

and the force exerted to remove the needle from the tissue. This experiment was repeated several times, and the average forces required to penetrate the tissue and dislodge the needle were found to be on average 3.86 mN and 10 mN respectively.

## 2.2 Computational Analysis of In-vivo Micropost Retention

With the determined force required to dislodge an anchored needle in the stomach lining, as well as confirmation that porcine tissue exhibits similar properties to that of the human stomach, a computational model was created to determine the ability of a self righting device with a hooked needle to retain its position in the human stomach. In addition, this model determined whether a self righting device with a variable number of ancillary bodies, which could be designed for various applications, would be capable of gastric retention.

According to literature, the characteristic fluid flow in the stomach has been found to be 2-3 mm/sec<sup>15</sup> while its Reynolds number has been determined to be on the order of 0.1 to 30<sup>16</sup>. This Reynolds number signifies that the flow within the stomach is laminar and is dominated by viscous forces. Stokes' law, a derivation of the Navier-Stokes equation modeled for small spherical objects in viscous fluids, can then be used to determine the drag force exerted on the device. This expression is shown in Equation 1, where F is the drag force, r is the radius of the device, v is the velocity of the liquid, and  $\mu$  is the dynamic viscosity of the liquid.

$$F = 6\pi * r * v * \mu \quad \text{Equation 1}$$

In order to use this equation, the dynamic viscosity of stomach acid must be found. According to literature, the dynamic viscosity of gastric acid can vary tremendously based on the

rheological properties of gastric digesta<sup>17</sup>. If a 10% glucose solution meal is ingested, the gastric contents can be modeled as a Newtonian fluid with a viscosity of  $10^{-3}$  Pa.s and density of 1 kg/L<sup>18 19</sup>. However, some foods have been shown to have viscosities as large as 10 Pa.s<sup>20</sup>. The introduction of even 1% of a more viscous food has been shown to increase the viscosity of gastric acid<sup>21</sup>. As a result, an average dynamic viscosity has been difficult to establish. However, for the purposes of this first-order simulation, an assumption was made that the food digested was glucose-based and therefore the dynamic viscosity is approximately  $10^{-3}$  Pa.s.

Using the radius of the self righting device that is attached to the needle of 4 mm, the Stokes' equation presented in Equation 1 can be used to determine the drag force exerted on the device. This drag force is established to be  $2.26 * 10^{-7}$  N, as shown using Equation 2.

$$F = 6\pi * 0.004 \text{ m} * 0.003 \text{ m/s} * 0.001 \text{ Pa.s} = 2.26 * 10^{-7} \text{ N} \quad \text{Equation 2}$$

As previously noted, since this force is significantly below the necessary force, as determined through the ex-vivo experiments using the Instron, to dislodge the device, it allows for the ability to attach separate, ancillary bodies to the self-righting device using surgical non-absorbable suture that could be used for a range of applications that shall be discussed in Chapter 4. Utilizing Equation 1 to calculate the drag force on these devices, which would likely have a maximum radius of 4.5 mm to fit comfortably in a 00 capsule, each device's drag force can be found to be  $2.54 * 10^{-7}$  N.

When determining the conditions required to dislodge the needle from the stomach lining, it is also important to consider torque. Utilizing the forces found for the self-righting

device and the ancillary bodies, the torque can be calculated using Equation 3, where  $\tau$  is torque,  $r$  is the moment arm, and  $F$  is force.

$$\tau = r \times F \tag{Equation 3}$$

Using this equation, where the moment arm is the needle’s length from the tissue to the bottom of the device (1.25 mm), a plot can then be created. As shown in Figure 5, a graph was created to compare the number of ancillary bodies attached to the self-righting device to the torque exerted by the drag force. However, as shown in this plot, even a device with 9 ancillary bodies would only experience torques several orders of magnitude smaller than what is needed to dislodge it.

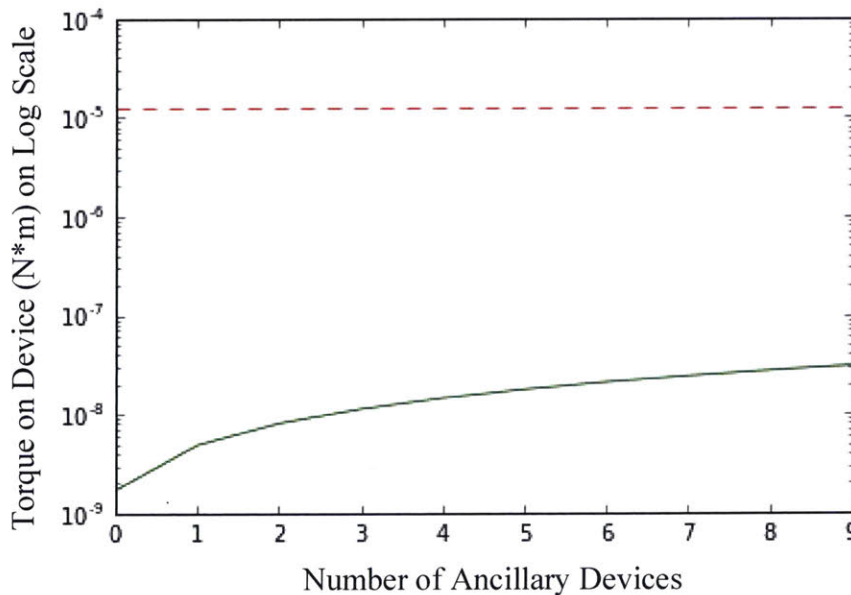


**Figure 5.** Graph describing the relationship between the number of ancillary bodies attached to the self righting device and the drag torque exerted on the system by the gastric acid. The dotted red line denotes the maximum torque that can be exerted on the system before the needle is dislodged. This value was determined from the force required to dislodge the needle in the ex-vivo experiments on the Instron, while using the needle’s length from the tissue to the bottom of the device of 1.25 mm as the moment arm.

From Figure 5, it can be determined that the drag torque remains several orders of magnitude smaller than the torque necessary to dislodge the device from the stomach lining. However, as noted earlier, since the dynamic viscosity does not account for food effects, a second model must be created. In the process of chewing, food is mashed into small spherical food boluses that then travel down the esophagus to the stomach. Once these boluses reach the stomach, they mix with gastric acid to form chyme<sup>22</sup>. Using sieving and laser diffraction measurements, studies have shown that across individuals these chewed particles can vary in size based on the texture of the foods ingested<sup>23 24</sup>. For example, raw vegetables create boluses that are on average larger than 2 mm<sup>25</sup>, whereas more than half of nut particles are less than 1 mm in diameter<sup>26</sup>.

Because of this large variation in the size of food boluses, a model was created to determine whether they could exert a large enough torque on impact with the self-righting device to dislodge it. It should be noted that this simulation was created with the assumption that no ancillary bodies were attached to the device, however, the needle would have to overcome the torque from the food boluses in addition to its own drag force. To do so, the food density was assumed to be  $1000 \frac{\text{kg}}{\text{m}^3}$  and that the boluses would compress on average 50% in a collision with the self-righting device while moving with the gastric acid at 3 mm/s. The lengths of the food boluses considered ranged from 0.1 mm to 100 mm to cover all possible diameters. However, as Figure 6 shows, even though the torque exerted by the food boluses can increase by an order of magnitude depending on their textures, the torques exerted on the self-righting device would still be far smaller than what would be required to dislodge it.



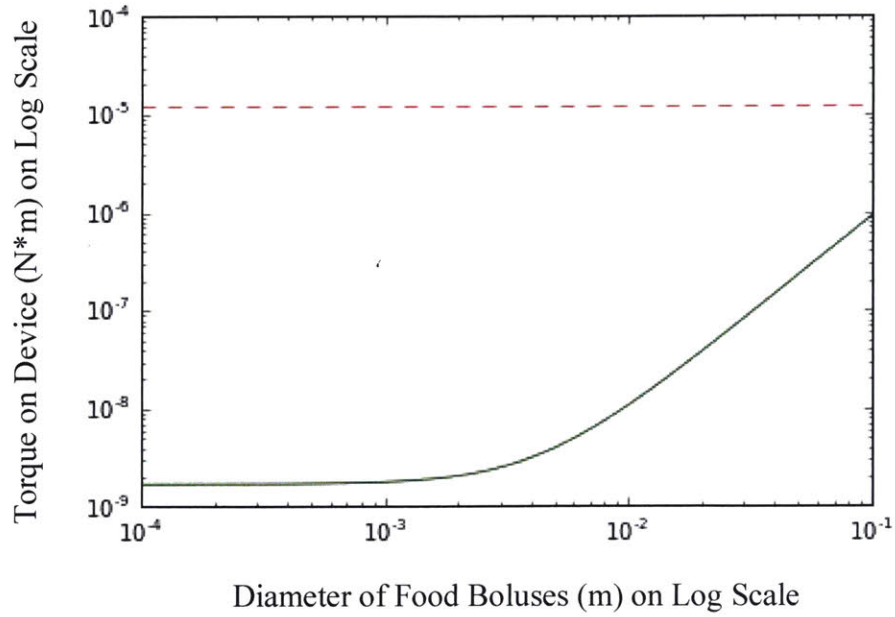


**Figure 6.** Graph comparing the size of the food boluses colliding with the self righting device and the torque exerted on it. The dotted red line denotes the maximum torque that can be exerted on the system before the needle is dislodged. This value was determined from the force required to dislodge the needle in the ex-vivo experiments on the Instron, while using the needle's length from the tissue to the bottom of the device of 1.25 mm as the moment arm.

### **3. EXPERIMENTAL VERIFICATION OF MICROPOST RETENTION**

With the preliminary measurements for the penetration depth and dislodgement forces determined, in addition to verification using computational simulations that the device could resist the forces present in the stomach, experiments were designed to test its retentive abilities. This chapter will discuss the in-vitro, as well as in-vivo, trials that were necessary to adequately simulate gastric conditions to determine whether the device can resist dislodgement.

#### **3.1 Synthetic Stomach Experiment**

In order to test the micropost's ability to retain its position in the stomach lining despite the effects of drag forces from the gastric flow, an in-vitro experiment was designed. To do so, Tygon PVC tubing were connected together to create a closed circuit attached to a water pump. A 10 cm by 10 cm section of tissue was dissected from the stomach of a Yorkshire pig and was fixed to the interior of tubing perpendicular to the ground. 3 self righting devices with hooked needles were then placed on top of this tissue. In addition, 3 self righting devices with unhooked needles, 3 self righting devices with no needle, and 3 spherical objects the same size as the self righting devices were also placed on the tissue as controls. Water was then introduced to the system and the pump was turned on to pump fluid at 0.1 m/s. Figure 7 illustrates how this experiment was conducted.

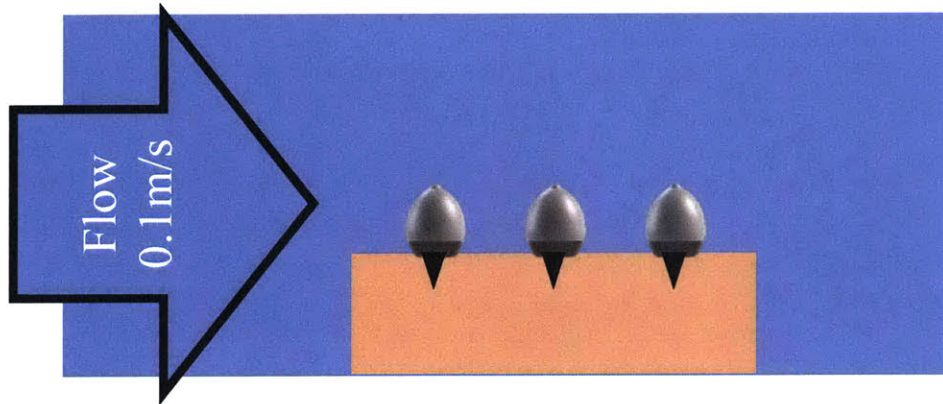


**Figure 7.** Illustration of the design of the in-vitro experiment conducted to determine the hooked needle’s ability to withstand fluid flow and associated drag forces.

The system was run for one week to determine the hooked needle’s ability to withstand fluid flow compared to its counterparts. As shown in Figure 8, while all the controls were dislodged by Day 2, the self-righting device with the hooked needle was able to retain its position for the entire week to verify the computational simulation’s results.

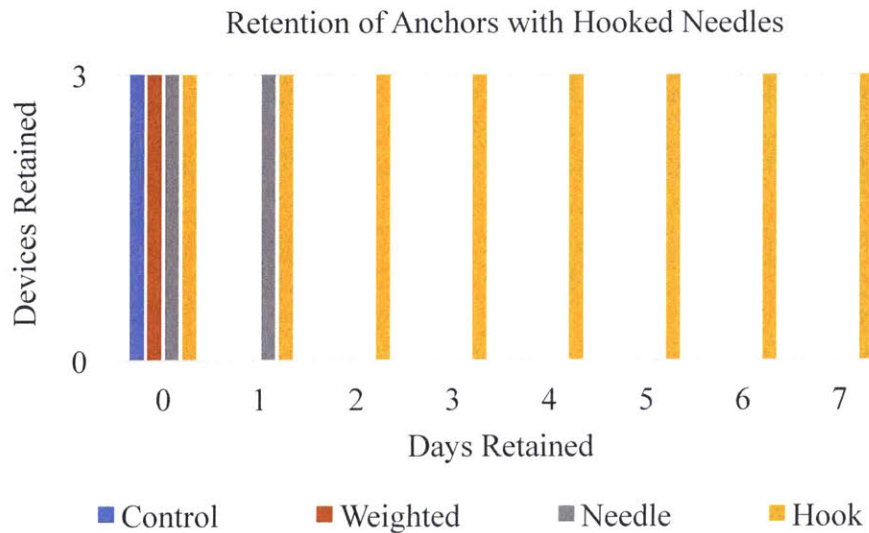


**Figure 8.** Graph of the results of the in-vitro experiment, which shows that the self-righting device with a hooked needle was the only device able to retain its position for the length of the experiment despite a strong fluid flow and associated drag forces.

### **3.2 In-vivo Trial Using Swine Model**

With the positive results from the synthetic stomach experiment that confirmed the predictions from the computational simulations, a multi-day in-vivo trial was designed for a swine model. Using an overtube, 4 self-righting devices with hooked needles were placed in a straight line on the right side of the stomach. Another 4 self-righting devices with regular needles were placed in a similar arrangement on the left side of the stomach so that they could be differentiated. On Days #2 and #3, an endoscope was used to monitor whether any of the self-righting devices had moved. However, when the experiment was conducted, all of the devices, whether hooked or unhooked, did not retain their position in the stomach.

There are several potential explanations for why the devices were dislodged in the pig stomach. In order to determine whether the device is not as resilient as the computational models predicted, further experiments must be conducted in-vitro to characterize its retentive ability. The protocols of several of these experiments will be described in Chapter 4. However, the dislodgement may also be due to the differences between the human stomach and the porcine model, such as motility. Unlike humans, which digest food between 1-4 hours in the stomach, pigs can take over 6 hours to pass their meal into the small intestine<sup>27</sup>. In addition, based on observation, pig boluses are much larger than their human counterparts, which would increase the force exerted on the device in a collision. Lastly, pigs eat large portions several times a day to keep their stomachs full, whereas humans exert more moderation in limiting their food intake.

## **4. CONCLUSIONS AND FUTURE WORK**

In conclusion, we have successfully characterized many of the properties involved with the long-term retention of microposts through preliminary experiments, as well as computational modeling. However, as the in-vivo trial in a pig indicated, there is still more work to be done to further identify what effects may have attributed to the dislodged hooked needles and design a new system to overcome them. As previously mentioned, this dislodgement may have been due to the differences in motility and food bolus size in pigs compared to humans. In order to solve this issue, it may be necessary to experiment with alternative diets for the pig models. However, once an in-vivo trial is successful, a range of different applications for long-term gastric retention will become possible and shall require further investigation.

### **4.1 Conclusions**

Through ex-vivo experiments on an Instron machine, the force required to penetrate the stomach lining, the depth necessary to ensure maximum retention, and the force required to remove a hooked needle were determined. A couple of computational models were created to utilize this data to verify the self righting device with a hooked needle would be able to retain its position despite the gastric conditions and associated effects it would be subject to. To simulate the drag forces, an in-vitro experiment was conducted to ensure the self-righting device would not be dislodged when exposed to fluid flows. With the positive results from this experiment, an in-vivo trial was conducted using a swine model, however, none of the hooked needles managed to retain their position over the multi-day investigation.

## 4.2 Future Experiments

Because of the negative results from the in-vivo trial, further experiments must be conducted to determine the effects that led to the hooked needles' dislodgement. One such experiment is to determine whether collisions with the food boluses caused the device to be displaced, despite the computational simulation's results. To do so, a protocol is being designed using a test meal recommended by the Food and Drug Administration for drug clinical trials<sup>28</sup>, that is grinded up to the size of food boluses. This meal will then be introduced to a beaker containing a piece of swine tissue that has been inserted with several self-righting devices that have hooked and unhooked needles. The system will then be placed in a laboratory shaker for a week. It shall be monitored every day to record whether the food boluses have dislodged the devices.

Another experiment that is to be conducted is to determine how much horizontal force can be exerted onto the self righting device before it is dislodged. To do so, a piece of swine tissue will be mounted parallel to the axis of movement of an Instron machine. A self-righting device with a hooked needle will then be inserted into the tissue. On the arm of the Instron, a stainless steel hooked needle adhered to a screw was secured in place, which will be lowered at a constant rate of 0.1 mm/sec until the device is dislodged. Since the Instron tracks the force exerted, the horizontal force necessary to dislodge the hooked needle will be determined.

Lastly, it has yet to be determined whether a multi-needle system would have a great likelihood of being retained in the stomach lining. Multiple systems must be created with 1, 2, 3, and 4 needles to be tested for their relative efficacy. In addition, the geometry of these needles in a plane must also be tested. For the three-needle system, equilateral and isosceles right triangles

will be tested. For four-needle system, a square and a rectangle with a 2:1 aspect ratio will be tested. Since this system is similar to ground anchors for homes in hurricane-prone areas that are subject to high wind speeds that can cause lateral movement, it is likely that more needles will improve long-term retention. In addition, as the Federal Emergency Management Agency (FEMA) recommends, anchors should be placed close to the edges of the ends of the building, which makes it likely that placing needles closer to the edge of the device could prevent it from dislodgement <sup>29</sup>.

### **4.3 Future Applications**

The long-term retention of microposts in the gastric lining could create a number of applications. As previously noted, it would allow for the prolonged delivery of medications that must traditionally be administered daily, such as insulin. It would also offer a viable method for biologic drugs, which traditionally must be injected due to enzymatic degradation in the gastric environment, to be delivered orally.

In addition, as discussed earlier in Chapter 2, microposts could serve as an anchor in the stomach for other devices that traditionally cannot maintain high residence times in the GI tract. These devices could be attached to the self-righting device using non-absorbable suture and sit in the stomach as ancillary bodies. One potential application could be for Bluetooth low energy for medical monitoring. This technology has created a growing field that promises to help doctors and health workers monitor their patient's condition at home <sup>30</sup>. A small Bluetooth monitor that could fit into a 00 capsule could thus be combined with a long-term needle retentive device to monitor different properties in the stomach, such as pH or temperature changes. Lastly, gastric electrical stimulation has been shown promise in dealing with several clinical problems, such as

gastroparesis and obesity<sup>31,32</sup>. If the ancillary bodies attached to the self-righting device were batteries in a multi-needle system was created, an electrical circuit could be created with the stomach lining that could facilitate this stimulation.



## 5. ACHKNOWLEDGEMENTS

The author would like to acknowledge Alex Abramson, Professor Giovanni Traverso, and Professor Robert Langer for their invaluable guidance and support throughout this project.

## 6. BIBLIOGRAPHY

1. Schoellhammer, C. M., Langer, R. & Traverso, G. Of microneedles and ultrasound: Physical modes of gastrointestinal macromolecule delivery. *Tissue Barriers* **4**, e1150235 (2016).
2. Giudice, E. L. & Campbell, J. D. Needle-free vaccine delivery. *Adv. Drug Deliv. Rev.* **58**, 68–89 (2006).
3. Sokolowski, C. J. & Giovannitti, J. A. Needle Phobia: Etiology, Adverse Consequences, and Patient Management. *Dent. Clin. North Am.* **54**, 731–744 (2010).
4. Dallel, N., Kacem, M., Nabouli, R. M. & El May, M. [Disposal of insulin syringes by diabetic patients. Report of 100 patients]. *Tunis. Med.* **83**, 390–2 (2005).
5. Miller, M. A. & Pisani, E. The cost of unsafe injections. *Bulletin of the World Health Organization* **77**, 808–811 (1999).
6. Osterberg, L. & Blaschke, T. Adherence to Medication. *N. Engl. J. Med.* **353**, 487–497 (2005).
7. Ingersoll, K. S. & Cohen, J. The impact of medication regimen factors on adherence to chronic treatment: a review of literature. *J. Behav. Med.* **31**, 213–224 (2008).
8. Traverso, G. *et al.* Microneedles for Drug Delivery via the Gastrointestinal Tract. *J. Pharm. Sci.* **104**, 362–367 (2015).
9. Kalantzi, L. *et al.* Characterization of the Human Upper Gastrointestinal Contents Under

- Conditions Simulating Bioavailability/Bioequivalence Studies. *Pharm. Res.* **23**, 165–176 (2006).
10. Vassallo, M. J., Camilleri, M., Prather, C. M., Hanson, R. B. & Thomforde, G. M. Measurement of axial forces during emptying from the human stomach. *Am. J. Physiol.* **263**, G230-9 (1992).
  11. Camilleri, M. & Prather, C. M. Axial forces during gastric emptying in health and models of disease. *Dig. Dis. Sci.* **39**, 14S–17S (1994).
  12. Anatomy Lesson #44: ‘Terrific Tunnel – GI System, Part 1’ |. Available at: <http://www.outlanderanatomy.com/anatomy-lesson-44-terrific-tunnel-gi-system-part-1/>. (Accessed: 3rd May 2017)
  13. Várkonyi, P. L. & Domokos, G. Static Equilibria of Rigid Bodies: Dice, Pebbles, and the Poincaré-Hopf Theorem. *J. Nonlinear Sci* **16**, 255–281 (2006).
  14. Guilloteau, P., Zabielski, R., Hammon, H. M. & Metges, C. C. Nutritional programming of gastrointestinal tract development. Is the pig a good model for man? (2017). doi:10.1017/S0954422410000077
  15. Kong, F. & Singh, R. P. Disintegration of Solid Foods in Human Stomach. doi:10.1111/j.1750-3841.2008.00766.x
  16. Abrahamsson, B. *et al.* A Novel in Vitro and Numerical Analysis of Shear-Induced Drug Release from Extended-Release Tablets in the Fed Stomach. doi:10.1007/s11095-005-5272-x
  17. Ferrua, M. J. & Singh, R. P. Modeling the fluid dynamics in a human stomach to gain insight of food digestion. *J. Food Sci.* **75**, R151-62 (2010).
  18. Schmidt, K. D., Abiodun, P. & Tolckmitt, W. Viscosity and electrolyte concentrations in

- gastric juice from cystic fibrosis children compared to healthy children. *Eur. J. Pediatr.* **136**, 193–7 (1981).
19. Bui, A. V. & Nguyen, M. H. Prediction of viscosity of glucose and calcium chloride solutions. *J. Food Eng.* **62**, 345–349 (2004).
  20. Steffe, J. F. *Rheological Methods in Food Process Engineering*. (Freeman Press, 1996).
  21. Rao, M. A. *Rheology of Fluid and Semisolid Foods*. (Springer US, 2007).  
doi:10.1007/978-0-387-70930-7
  22. Thomas, A. Gut motility, sphincters and reflex control. *Anaesth. Intensive Care Med.* **7**, 57–58 (2006).
  23. Hoebler, C., Devaux, M. F., Karinthe, A., Belleville, C. & Barry, J. L. Particle size of solid food after human mastication and in vitro simulation of oral breakdown. *Int. J. Food Sci. Nutr.* **51**, 353–66 (2000).
  24. Foster, K. D., Woda, A. & Peyron, M. A. Effect of Texture of Plastic and Elastic Model Foods on the Parameters of Mastication. *J. Neurophysiol.* **95**, 3469–3479 (2006).
  25. Peyron, M.-A., Mishellany, A. & Woda, A. Particle Size Distribution of Food Boluses after Mastication of Six Natural Foods. *J. Dent. Res.* **83**, 578–582 (2004).
  26. Jalabert-Malbos, M.-L., Mishellany-Dutour, A., Woda, A. & Peyron, M.-A. Particle size distribution in the food bolus after mastication of natural foods. *Food Qual. Prefer.* **18**, 803–812 (2007).
  27. Gregory, P. C., McFadyen, M. & Rayner, D. V. Pattern of gastric emptying the pig: relation to feeding. *Br. J. Nutr.* **64**, 45–58 (1990).
  28. Administration, D. Food-Effect Bioavailability and Fed Bioequivalence Studies. (2002).
  29. *Understanding and Improving Performance of New Manufactured Homes During High-*

*Wind Events*. (2007).

30. Omre, A. H. Bluetooth low energy: wireless connectivity for medical monitoring. *J. Diabetes Sci. Technol.* **4**, 457–63 (2010).
31. ZHANG, J. & CHEN, J. D. Z. Systematic review: applications and future of gastric electrical stimulation. *Aliment. Pharmacol. Ther.* **24**, 991–1002 (2006).
32. Abell, T. *et al.* Gastric Electrical Stimulation for Medically Refractory Gastroparesis. doi:10.1016/S0016-5085(03)00878-3